Modeling and Simulation of Aircraft Motion on the Ground: Part I. Derivation of Equations of Motion

Kapseong Ro* and Haechang Lee*
Aircraft Division
Korea Aerospace Research Institute
P.O. Box 113, Taejon, Korea 305-600

Abstract

Developed in these two series of paper is a complex dynamic model representing the motion of aircraft on the ground and a computer program for numerical simulation. The first part of paper presents the theoretical derivation of equations of motion of the landing gear system based on the physical principle. Developed model is 'structured' in the sense that the undercarriage system is regarded as an assembly of strut, tire, and wheel, where each component is modeled by a separate module. These modules are linked with two external modules - the aircraft and the runway characteristics - to carry out dynamic analysis and numerical simulation of the aircraft motion on the ground. Three sets of coordinate system associated with strut, wheel/tire and runway are defined, and external loads to each component and response characteristics are examined. Lagrangian formulation is used to derive the undercarriage equations of motion relative to the moving aircraft, and the resultant forces and moments from the undercarriage are transformed to aircraft body axes.

Key Word : Modeling and Simulation, Aircraft Ground Motion, Landing Gear

NORMENCLATURE

F_E, F_{RW}	:	Earth-surfaced and Runway reference frames
F_B, F_V	:	Body and Vehicle-carried-vertical reference frames
F_{SS}, F_{WH}	:	Shock Strut and Wheel reference frames
F_{WV}	:	Wheel/Tire Velocity reference frames
B^*	:	Origin of Body frame, F_B
$O_A X_A Y_A Z_A$	:	A Cartesian coordinates of reference frame, F_A
$\vec{R}^{XY}$	:	Position vector from a point X to a point Y
${}^Y\vec{V}^X$	:	Velocity of point X in a reference frame F_Y
$\vec{X}_Y$	:	Components expression of a vector in a cartesian coordinates of F_Y
$\frac{{}^Y d}{dt}\vec{X}$	:	Derivative of a vector $\vec{X}$ in a reference frame F_Y
L_{XY}	:	Transformation matrix from a reference frame, F_Y, to a reference frame, F_X
L_1, L_2, L_3	:	Matrices of three successive, simple rotation for a transformation matrix (e.g. Euler angles transformation as defined in Reference 1)

* Senior Researcher
E-mail : kapseong@yahoo.com, TEL : 042-860-2343, FAX : 042-860-2006

$\mathbf{cv}(\vec{X}_Y)$: Skew symmetric matrix form of a vector, i.e. $\mathbf{cv}(\vec{X}_Y) = \begin{bmatrix} 0 & -x_3 & x_2 \\ x_3 & 0 & -x_1 \\ -x_2 & x_1 & 0 \end{bmatrix}$

Introduction

The motion of aircraft on the ground is significantly different from that of airborne. It stems from complex interactions among the dynamics of aircraft, the undercarriage system and the runway. Developing a representative mathematical model involves quite a laborious process, especially for the undercarriage system dynamics. The undercarriage system exhibits much faster dynamic characteristics than the whole aircraft motion. It can be modeled to different levels of details, ranging from a simple second order model for quantitative behavior to a sophisticated, modularized model to study the complex ground handling qualities with parametric analysis of the system.

The appropriate model should be carefully developed by considering the task objective and available computing resources for simulation. In case of training simulators, simple undercarriage models are usually adopted because the majority of training is used for in-flight operations comparing to a little time spent on the ground operations. However, these simple models are inadequate for engineering simulation where the comprehensive ground handling characteristics and the system acceptability must be tested and evaluated. In the real-time simulation environment such as a flight simulator, the details of model are restricted by computing power so that the typical undercarriage models used in the real-time simulation are functionally limited for use with an engineering simulator.[2][3] Meanwhile, those models and simulation code used for engineering analysis and system design[4][5] may not seem to be suitable for real-time operations due to their complexity.[6]

With the advent of high performance but low cost computing hardware and powerful software, a real-time simulation has become a practical solution for the undercarriage system design and the ground handling qualities study. Also, a standardized analytical modeling capabilities that are comprehensive but not cumbersome are sought.[7] This paper presents a genuine work of developing a dynamic model of aircraft undercarriage and the ground roll characteristics suitable for engineering analysis and possibly for real-time simulation. The model developed is 'structured' in the sense that the undercarriage system is regarded as an assembly of strut, tire and wheel, where each component is modeled by a separate module. This allows investigating the effects of component level changes, such as tire pressure, strut damping, etc., upon the overall undercarriage system responses and the ground handling properties.

Model Structure

Figure 1 shows a schematic diagram of the mathematical model of the aircraft motion on the ground. The flow starts by importing input data from the aircraft module including the aircraft position, height, ground velocities, attitude angles, and so on. Next, in the strut module, strut deflection and rates are computed using the aircraft C.G. and in turn strut spring and damping forces are calculated. In the runway module, runway properties such as surface conditions and slop can be introduced. The tire module takes inputs from the strut and the runway module to compute forces in undercarriage axes by using the longitudinal and lateral friction coefficients between the tire and the ground. Also, the effects of braking and nose wheel steering forces may be introduced in this module. In the wheel module, the computed forces in the tire module are transformed into the aircraft body axes and the corresponding undercarriage moments are calculated. The resultant forces and moments are then returned to the aircraft module.

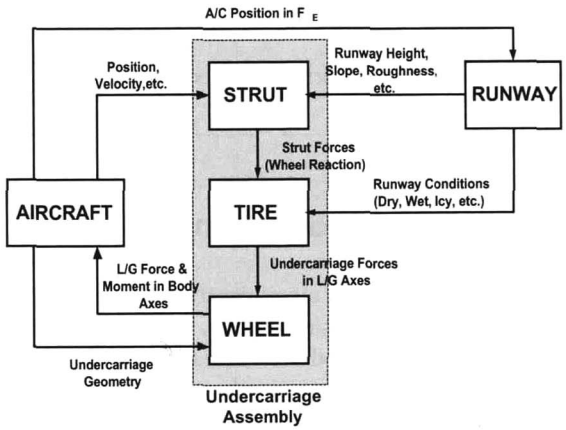

Fig. 1. Undercarriage and Ground Roll Model Structure

Model Development

The first step in mathematical modeling of a dynamic system is to define a set of axis systems and notations. Two coordinate systems are defined associated with each undercarriage system, one with the strut, denoted by F_{SS} and the other with the wheel, denoted by F_{WH}. The origin O_{SS} of F_{SS} is at the hinge point of shock strut to the aircraft body, P_{SS} as shown in Figure 2, and $O_{SS}Z_{SS}$ is directed downward along the shock strut axis, $O_{SS}X_{SS}$ is directed forward along the shock strut axis of rotation, and $O_{SS}Y_{SS}$ is directed to the right to the plane $C_{X_{SS}Z_{SS}}$ to complete a Cartesian coordinate system. The origin O_{WH} of F_{WH} is at the hinge point of wheel to shock strut, P_W, with $O_{WH}Z_{WH}$ directed downward along the shock strut

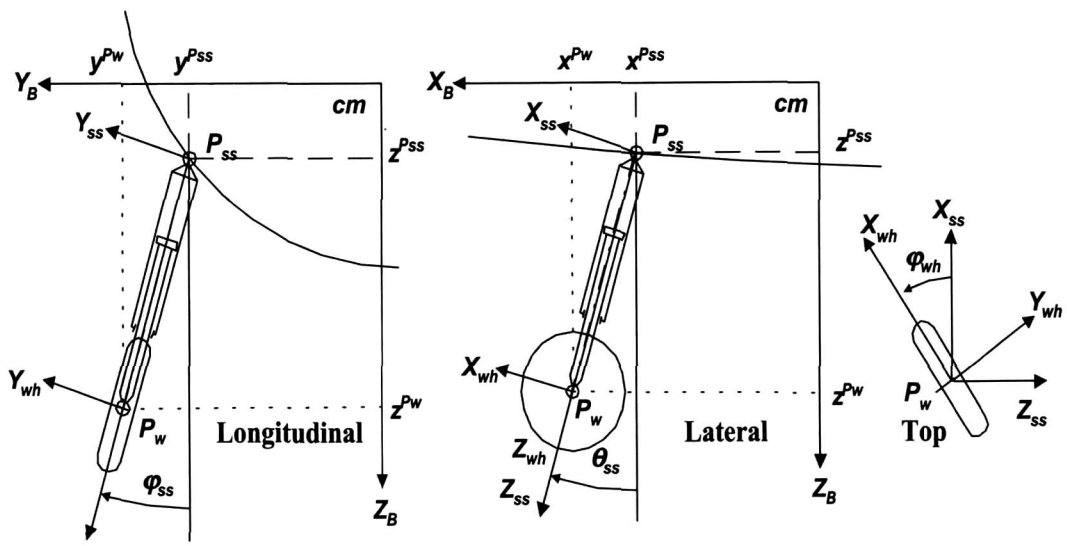

Fig. 2. Strut & Wheel Coordinates

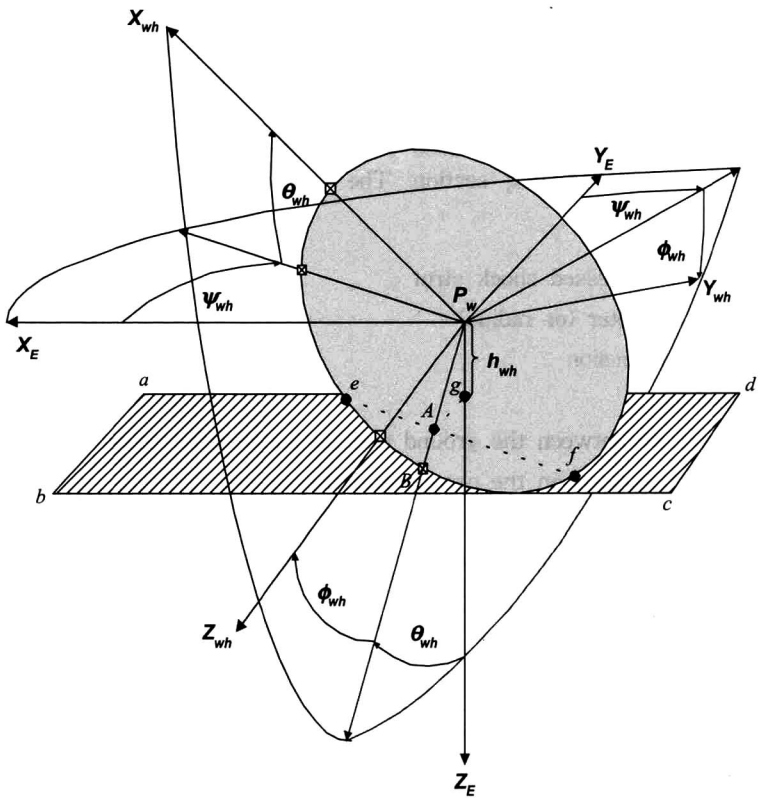

Fig. 3. Wheel Orientation Angles relative to Runway

axis, i.e. coinciding with $O_{SS}Z_{SS}$, and $O_{WH}X_{WH}$ in the wheel plane directing forward perpendicular to $O_{WH}Z_{WH}$, and $O_{WH}Y_{WH}$ directed along the wheel axis of rotation to complete a Cartesian coordinate system. A coordinate system associated with the runway is also defined and denoted by F_{RW}, which differs by the runway heading angle Ψ_{RW} from the local earth frame, F_E. Now, the angles for the orientation of the shock strut and the wheel can be defined as shown in Figures 2 and 3, where

ϑ_{ss} : Inclination angle between shock strut and O_BZ_B axis, i.e. $\measuredangle(O_BZ_B, O_{SS}Z_{SS})$

φ_{ss} : Inclination angle between shock strut and the plane of symmetry $C_{X_BZ_B}$

φ_{wh} : Nose wheel steering angle

$\phi_{wh}, \theta_{wh}, \psi_{wh}$: Euler angles from F_{RW} to F_{WH}

Using the angles defined above, the coordinate transformation matrices, $L_{SS\cdot WH}$ from F_{WH} to F_{SS}, $L_{SS\cdot B}$ from F_B to F_{SS}, and $L_{WH\cdot RW}$ from F_{RW} to F_{WH}, can be determined as follows:

$$L_{SS\cdot WH} = L_1(0)L_2(0)L_3(\varphi_{wh}) = L_3(\varphi_{wh}) \tag{1.a}$$

$$L_{SS\cdot B} = L_1(-\varphi_{ss})L_2(\vartheta_{ss})L_3(0) = L_1(-\varphi_{ss})L_2(\vartheta_{ss}) \tag{1.b}$$

$$L_{WH\cdot RW} = L_1(\phi_{wh})L_2(\theta_{wh})L_3(\psi_{wh}) \tag{1.c}$$

1. Kinematics

The kinematics of P_{SS}, P_W, and P_A, i.e. the point of contact between wheel and runway, are of interests because these points are associated with the shock strut deflection and its rate, and tire deflection. These quantities are used to compute forces and moments acting on the strut and the wheel in the following section. The characteristic lengths shown in Figure 4 represents as follows:

$l_{ss,o}$: Length of uncompressed shock strut
d_{wh} (or r_{wh}) : Wheel diameter (or radius)
x_p : Oleo strut compression
δ_{tire} : Tire deflection
h_{wh} : Vertical distance between the ground and the hinge point of wheel P_w
h_{cm} : Vertical distance between the ground and the aircraft C.G.

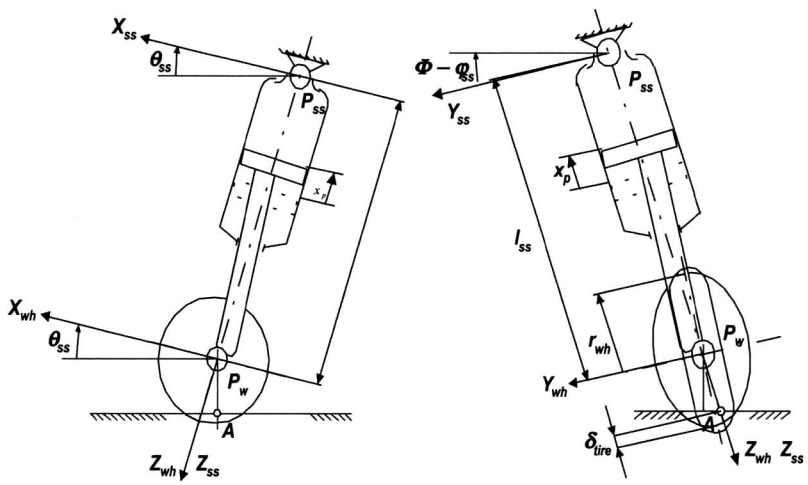

Fig. 4. Definitions for Characteristic Lengths

The position vectors $\vec{R}^{B^*P_{SS}}$, $\vec{R}^{B^*P_W}$, $\vec{R}^{B^*P_A}$ and their coordinates in F_B are defined as

$$\vec{R}\,{}_B^{B^*P_{SS}} = \begin{bmatrix} x^{P_{SS}} \\ y^{P_{SS}} \\ z^{P_{SS}} \end{bmatrix}, \quad \vec{R}\,{}_B^{B^*P_W} = \begin{bmatrix} x^{P_W} \\ y^{P_W} \\ z^{P_W} \end{bmatrix}, \quad \vec{R}\,{}_B^{B^*P_A} = \begin{bmatrix} x^{P_A} \\ y^{P_A} \\ z^{P_A} \end{bmatrix} \tag{2}$$

and it is immediate that

$$\vec{R}\,{}_{SS}^{P_{SS}P_W} = [\,0 \;\; 0 \;\; (l_{ss,o} - x_p)\,]^T \tag{3}$$

Now, consider $\vec{R}^{B^*P_W} = \vec{R}^{B^*B_o^*} + \vec{R}^{B_o^*P_{SS}} + \vec{R}^{P_{SS}P_W}$ where B_o^* is the C.G. position at the middle of its range of variation. Expressing it in terms of F_B coordinate,

$$\vec{R}_{B}^{B^*P_W} = \vec{R}_{B}^{B^*B_o^*} + \vec{R}_{B}^{B_o^*P_{SS}} + L_{B\cdot SS}\vec{R}_{SS}^{P_{SS}P_W} = \vec{R}_{B}^{B^*B_o^*} + \vec{R}_{B}^{B_o^*P_{SS}} + L_2^T(\vartheta_{ss})L_1^T(-\varphi_{ss})\vec{R}_{SS}^{P_{SS}P_W} \tag{4}$$

Also, $\vec{R}^{O_EP_W} = \vec{R}^{O_EB^*} + \vec{R}^{B^*P_W}$ and expressing it in terms of F_E components,

$$\vec{R}_{E}^{O_EP_W} = \vec{R}_{E}^{O_EB^*} + L_{EV}L_{VB}\vec{R}_{B}^{B^*P_W} \tag{5}$$

Substituting (4) into (5) leads to

$$\vec{R}_{E}^{O_EP_W} = \vec{R}_{E}^{O_EB^*} + L_3^T(\Psi)L_2^T(\Theta)L_1^T(\Phi)\left\{\vec{R}_{B}^{B^*B_o^*} + \vec{R}_{B}^{B_o^*P_{SS}} + L_2^T(\vartheta_{ss})L_1^T(-\varphi_{ss})\vec{R}_{SS}^{P_{SS}P_W}\right\} \tag{6}$$

It is evident that the z component of $\vec{R}_{E}^{O_EP_W}$ and $\vec{R}_{E}^{O_EB^*}$ are $-h_{wh}$ and $-h_{cm}$, respectively, so that the z component of (6) can be represented as follows:

$$\begin{aligned} h_{wh} = h_{cm} + & \left\{\left(\Delta x_{cg}\,\bar{c}_{mac} + x^{P_{ss,o}}\right) + (l_{ss,o} - x_p)\cos\varphi_{ss}\sin\vartheta_{ss}\right\}\sin\Theta - \\ & \left\{\left(\Delta y_{cg}\,\bar{c}_{mac} + y^{P_{ss,o}}\right) + (l_{ss,o} - x_p)\sin\varphi_{ss}\right\}\cos\Theta\sin\Phi - \\ & \left\{\left(\Delta z_{cg}\,\bar{c}_{mac} + z^{P_{ss,o}}\right) + (l_{ss,o} - x_p)\cos\varphi_{ss}\cos\vartheta_{ss}\right\}\cos\Theta\cos\Phi \end{aligned} \tag{7}$$

From Figures 3 and 4, the tire deflection δ_{tire} can be expressed as

$$\delta_{tire} = r_{wh} - |\vec{R}^{P_WA}| = \begin{cases} r_{wh} - \left(\dfrac{h_{wh}}{\cos\phi_{wh}}\right), & r_{wh} > \left(\dfrac{h_{wh}}{\cos\phi_{wh}}\right) \\ 0, & r_{wh} < \left(\dfrac{h_{wh}}{\cos\phi_{wh}}\right) \end{cases} \tag{8}$$

It is of interest to compute the angle, ϕ_{wh} in terms of known angles including φ_{ss}, ϑ_{ss}, φ_{wh} and the aircraft attitude angles, Φ, Θ, Ψ. This can be obtained from the following relation.

$$L_{WH\cdot RW} = L_{WH\cdot SS}L_{SS\cdot B}L_{B\cdot V}L_{V\cdot RW} \tag{9}$$

Assuming that the runway heading angle Ψ_{RW} equals to zero such that $L_{V\cdot RW} = I$ (i.e. runway is heading the North), and expanding and extracting the l_{13}, l_{33} elements of the equation (9) results in the following relations.

$$\begin{aligned} -\sin\theta_{wh} = & -(\cos\varphi_{wh}\cos\vartheta_{ss} + \sin\varphi_{wh}\sin\varphi_{ss}\sin\vartheta_{ss})\sin\Theta \\ & -\sin\varphi_{wh}\cos\varphi_{ss}\sin\Phi\cos\Theta \\ & +(-\cos\varphi_{wh}\sin\vartheta_{ss} + \sin\varphi_{wh}\sin\varphi_{ss}\cos\theta_{ss})\cos\Phi\cos\Theta \end{aligned} \tag{10.a}$$

$$\cos\phi_{wh}\cos\theta_{wh} = -\cos\varphi_{ss}\sin\vartheta_{ss}\sin\Theta + \sin\varphi_{wh}\sin\Phi\cos\Theta + \cos\varphi_{ss}\cos\theta_{ss})\cos\Phi\cos\Theta \tag{10.b}$$

Computing (10.a) and (10.b) sequentially finds the value of $\cos\phi_{wh}$, which enables to compute the tire deflection by (8). After computing the tire deflection, the position vector from the aircraft C.G. to the wheel/ground contact point can be obtained. It will be shown in the following section that this position vector is used to compute the applied moment to the aircraft C.G. by the contact forces between the landing gear and the ground. From (8), it can be recognized that the magnitude of $\vec{R}^{P_WP_A}$ can be expressed as $(r_{wh} - \delta_{tire})$ while its direction

is along $O_{RW}Z_{RW_2}$, which is the z-axis of the second intermediate frame of the transformation matrix $L_{WH\cdot RW}$. Therefore, from the vector relation of $\vec{R}^{B^*A} = \vec{R}^{B^*P_w} + \vec{R}^{P_wA}$, and representing it in terms of F_B coordinate leads to the following equation.

$$\begin{bmatrix} x^{P_A} \\ y^{P_A} \\ z^{P_A} \end{bmatrix} = \begin{bmatrix} x^{P_w} \\ y^{P_w} \\ z^{P_w} \end{bmatrix} + L_{B\cdot SS} L_{SS\cdot WH} L_1(\phi_{wh}) \begin{bmatrix} 0 \\ 0 \\ r_{wh} - \delta_{tire} \end{bmatrix} \tag{11}$$

One of important kinematic variables is the wheel side-slip angle, denoted by β_{wh} in Figure 5, which is required to compute the forces acting on the wheel/tire from the runway surface. This angle depends on the velocity of P_W in F_E, which is obtained by

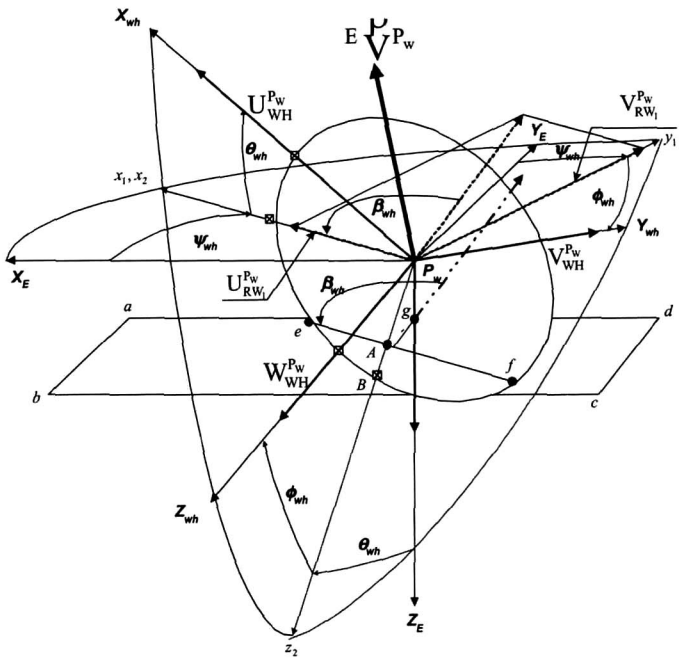

Fig. 5. Wheel Sideslip Angle Definition

$$\frac{^E d}{dt}\vec{R}^{O_E P_W} = \frac{^E d}{dt}\vec{R}^{O_E B^*} + \frac{^B d}{dt}\vec{R}^{B^* P_W} + {}^N\vec{\omega}^B \times \vec{R}^{B^* P_W} \tag{12}$$

Since $\frac{^B d}{dt}\vec{R}^{B^* P_W} = 0$ for the motion on the ground, the velocity $^E\vec{V}^{P_W}$ is given by

$$^E\vec{V}^{P_W} = {}^E\vec{V}^{B^*} + {}^E\vec{\omega}^B \times \vec{R}^{B^* P_W} \tag{13}$$

Representing (13) in terms of the body axes gives

$$^E\vec{V}^{P_W}_B = {}^E\vec{V}^{B^*}_B + \mathbf{cv}\left({}^E\vec{\omega}^{B^*}_B\right)\vec{R}^{B^* P_W}_B \tag{14.a}$$

$$\begin{bmatrix} U^{P_w} \\ V^{P_w} \\ W^{P_w} \end{bmatrix} = \begin{bmatrix} U \\ V \\ W \end{bmatrix} + \begin{bmatrix} 0 & -R & Q \\ R & 0 & -P \\ -Q & P & 0 \end{bmatrix} \begin{bmatrix} x^{P_w} \\ y^{P_w} \\ z^{P_w} \end{bmatrix} \tag{14.b}$$

where U, V, W, P, Q, R represent the aircraft linear and angular velocities in the body axes, respectively. As seen in the Figure 6, the wheel side-slip angle is found from the first intermediate frame of the transformation matrix $L_{WH \cdot RW}$, so that it is necessary to transform (14) into that frame as follows:

$$\begin{aligned} {}^{E}\vec{V}^{P_w}_{RW_1} &= L_{RW_1 \cdot WH} L_{WH \cdot B}\, {}^{E}\vec{V}^{P_w}_{B} \\ &= L_{RW_1 \cdot RW_2} L_{RW_2 \cdot WH}\, L_{WH \cdot SS} L_{SS \cdot B}\, {}^{E}\vec{V}^{P_w}_{B} \\ &= L_2^T(\theta_{wh}) L_1^T(\phi_{wh}) L_3^T(\varphi_{wh}) L_1(-\varphi_{ss}) L_2(\vartheta_{ss})\, {}^{E}\vec{V}^{P_w}_{B} \end{aligned} \tag{15}$$

Let us denote

$${}^{E}\vec{V}^{P_w}_{RW_1} = \begin{bmatrix} U^{P_w}_{RW_1} & V^{P_w}_{RW_1} & W^{P_w}_{RW_1} \end{bmatrix}^T \tag{16}$$

then, the wheel-side slip angle is computed by

$$\beta_{wh} = \tan^{-1}\left(\frac{V^{P_w}_{RW_1}}{U^{P_w}_{RW_1}} \right) \tag{17}$$

2. Analytic Model

The kinematic variables computed in the previous section allow to compute the forces acting on the undercarriage assembly, which is modeled as a composition of strut, wheel and tire. The models of those forces acting on each component of undercarriage assembly are discussed as below.

Strut Model

The strut is typically modeled as a single chamber cantilevered oleo-pneumatic shock absorber, as shown in Figure 6. The forces acting on the strut can be characterized as three kinds. There is the pneumatic static compression forces, denoted by $\vec{F}^{sp}$, acting on the strut. Its magnitude depends upon the amount of strut compression displacement, x_p, being positive in compression. Secondly, there is the hydraulic damping force, denoted by $\vec{F}^{sh}$, along the strut. Its direction is opposite to the motion of the piston/rod. Thirdly, there are frictional forces, $\vec{F}^{sf}$ created as bearing surfaces slide relative to each other during strut motion. Through these three mechanism, the forces are transmitted from the lower strut which is attached to the wheel/tire, to the upper strut which is attached to the aircraft. These are internal forces that occur as equal and opposite pairs as they act on the upper and lower section of the strut.

Wheel/Tire Model

A typical, widely-used tire model is a point contact spring model with either linear or nonlinear stiffness and damping in parallel. Using the point contact follower model, the forces can be characterized as the normal force, $\vec{F}^{n}$, the wheel-side force, $\vec{F}^{r}$, and the wheel drag

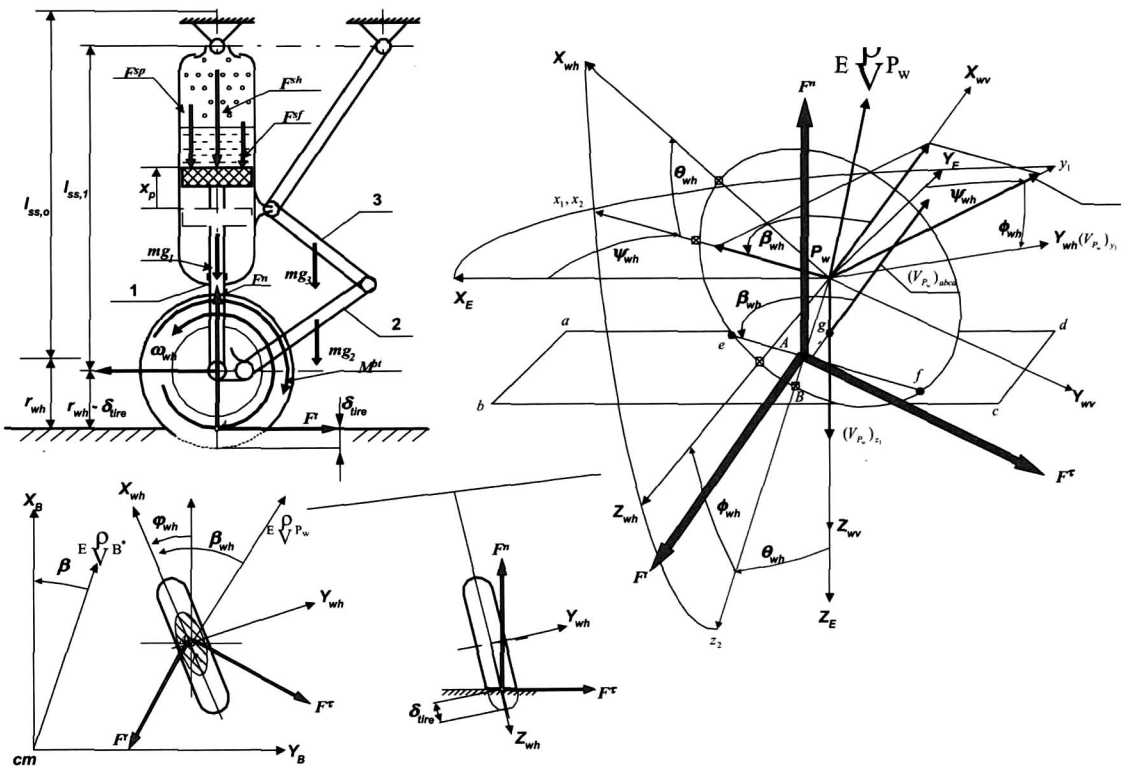

Fig. 6. Forces acting on Undercarriage Assembly

force, $\vec{F}^t$. The normal force is along the local vertical in upward direction, and its magnitude depends on the amount of tire deflection, δ_{tire}, with

$$F^n = \begin{cases} 0, & |\vec{R}^{P_wA}| \geq r_{wh} \\ f(\delta_{tire}), & |\vec{R}^{P_wA}| < r_{wh} \end{cases} \tag{18}$$

The wheel side-force lies on the contact plane between the wheel/tire and the runway surface. Its direction is perpendicular to the sum of velocity vector $U^{P_w}_{RW_1}$ and $V^{P_w}_{RW_1}$ (see Figure 5), and its magnitude depends upon the coefficient of sliding friction, $C_{y_{tire}}(\beta_{wh})$ and the normal force by the following relation:

$$F^\tau = C_{y_{tire}}(\beta_{wh})\, F^n(\delta_{tire}) \tag{19}$$

The wheel drag force lies on the contact plane between the tire and the runway surface. Its direction is opposite to the sum of velocity vector $U^{P_w}_{RW_1}$ and $V^{P_w}_{RW_1}$, and its magnitude depends upon the rolling coefficient of friction k_d by the following relation:

$$F^t = k_d F^n(\delta_{tire}) \tag{20}$$

where for rolling without slipping case,

$$k_d = \left[k_{d,0} + \frac{M^{bt}}{F^n(\delta_{tire})(r_{wh} - \delta_{tire})} \right] \ (\leq k_{d,\max}) \tag{21}$$

and $k_d = k_{d,\max}$ for slipping and rolling case. The values of $k_{d,0}$, and $k_{d,\max}$ depend upon the runway surface conditions such as dry, damp, wet, icy, concrete, asphalt, unpaved, etc. M^{bt} represents the applied brake torque on the main wheel axis of rotation. It comprises from the manual brake operation by the pilot and the first-officer through their brake pedals. In addition, there is an automatic anti-skid brake system which provides the wheel lock protection at touchdown and skid-protection for the manual brake operation. In case of rejected take-off situation, the thrust levers are retracted but the ground speed still remains above some value so that the anti-skid system activates with the maximum brake pressure. It will be de-activated when the airplane completely stops or manually disengaged. For landing phase just after touchdown with the thrust levers all retracted, it activates with a selected level of brake pressure until the airplane completely stops or manually disengaged. The pilot can de-activate the automatic brake operation in any case of take-off and landing mode when he operates the brake pedal; advances the thrust lever; and/or switches the selector off.

3. Equations of Motion

Each undercarriage assembly can be idealized as being composed of three mechanical parts of strut, mechanical linkages and wheel/tire. It is advantageous to formulate the governing equations of motion using Lagrange's equations of motion given by

$$\frac{d}{dt}\left(\frac{\partial T_{rel}}{\partial \dot{q}_i}\right) - \left(\frac{\partial T_{rel}}{\partial q_i}\right) + \left(\frac{\partial U}{\partial \dot{q}_i}\right) = Q_i \tag{22}$$

where q_i is a generalized coordinate, T_{rel} is the kinetic energy of the motion of undercarriage assembly relative to the body reference frame, U is the potential energy, and Q_i is the generalized external force. Since the coordinates are measured in the body frame, which is non-Newtonian by virtue of aircraft motion, an appropriate modification must be made to the external force field acting on the system when calculating the generalized forces.[1]

Energy of Relative Motion & EOM

The motion of interest for the main gear is the piston stroke and the angular displacement of the wheel, so that the generalized coordinate for the main gear can be chosen as $q_1 = x_p$ and $q_2 = \mu_{wh}$. In case of the telescopic nose gear one additional degree of freedom should be allowed for the wheel steering angle. Since there is no potential energy term in the Lagrange's equation of motion for landing gear, (22) becomes

$$\frac{d}{dt}\left(\frac{\partial T_{rel}}{\partial \dot{q}_i}\right) - \left(\frac{\partial T_{rel}}{\partial q_i}\right) = Q_i \tag{23}$$

and the kinetic energy of relative motion for a main gear assembly can be expressed as

$$T_{rel} = T_p + T_{wh} + T_2 + T_3 \tag{24}$$

where T_p, T_{wh}, T_2, T_3 are the kinetic energies of the strut motion, the wheel/tire motion, and mechanical linkages motion relative to the body frame, respectively. The total kinetic energy (see Appendix) of undercarriage relative motion is given by

$$T_{rel}=\left\{m_p+m_{wh}+\frac{m_2[14l_2^2-3(a_{2,0}-x_p)^2]}{6[4l_2^2-(a_{2,0}-x_p)^2]}+\frac{m_3l_3^2}{3[4l_3^2-(a_{2,0}-x_p)^2]}\right\}\frac{\dot{x}_p^2}{2}+\frac{J_{wh}\dot{\mu}_{wh}^2}{2} \tag{25}$$

Now, substituting (25) into (23) and evaluating for $q_1=x_p$ and $q_2=\mu_{wh}$ leads to

$$\begin{aligned}&\left\{m_p+m_{wh}+\frac{m_2[14l_2^2-3(a_{2,0}-x_p)^2]}{6[4l_2^2-(a_{2,0}-x_p)^2]}+\frac{m_3l_3^2}{3[4l_3^2-(a_{2,0}-x_p)^2]}\right\}\ddot{x}_p-\\&\left\{\frac{m_2l_2^2(a_{2,0}-x_p)}{3[4l_2^2-(a_{2,0}-x_p)^2]}+\frac{m_3l_3^2(a_{2,0}-x_p)}{3[4l_3^2-(a_{2,0}-x_p)^2]}\right\}\dot{x}_p^2=Q_1\end{aligned} \tag{26.a}$$

$$J_{wh}\ddot{\mu}_{wh}=Q_2 \tag{26.b}$$

Evaluation of Generalized Forces

Consider P_i be the center of mass of the strut (i=1), the mechanical linkage (i=2,3), and the wheel/tire (i=4), respectively, as shown in Figure 6. Now, the vector equation, $\vec{R}^{O_EP_i}=\vec{R}^{O_EB^*}+\vec{R}^{B^*P_i}$ holds true, and the inertial acceleration is given by

$$\vec{a}^{E\,P_i}=\vec{a}^{E\,B^*}+\vec{a}^{B\,P_i}+\left(\vec{\alpha}^{E\,B}\times\vec{R}^{B^*P_i}\right)+\left(\vec{\omega}^{E\,B}\times\vec{\omega}^{E\,B}\times\vec{R}^{B^*P_i}\right)+\left(2\,\vec{\omega}^{E\,B}\times\vec{V}^{B\,P_i}\right) \tag{27}$$

Applying the Newton's equation of motion in the aircraft body reference frame leads to

$$m_i\vec{a}^{E\,P_i}=\vec{F}^{i}+\vec{I}^{E_i}+\vec{I}^{C_i} \tag{28}$$

where m_i is the mass of the i^{th} mechanical part, $\vec{F}^{i}$ is the sum of external force applied, $\vec{I}^{E_i}$ represents the transient force due to the motion of aircraft, and $\vec{I}^{C_i}$ represents the Coriolis' force due to the motion of aircraft. For a practical use of undercarriage equation of motion operating on the ground, the magnitude of applied external force is much greater than the transient and the Coriolis' force so that the effect of those forces can be usually neglected. Now, the generalized forces can be evaluated from the principle of virtual work,

$$Q_i=\frac{\delta W}{\delta q_i} \tag{29}$$

where δW is the work done by all the external forces and moments through a virtual displacement δq_i. The virtual displacement (linear) δx_p is in the direction of $O_{ss}Z_{ss}$ axis, while $\delta\mu_{wh}$ is in the (rotational) direction of $O_{wh}Y_{wh}$ axis. It is convenient to express the external forces in components of F_{SS}, while the external moments are in F_{WH}. Then, the forces acting on the strut in F_{SS} components can be simply written as

$$\vec{F}^{\,s}_{SS}=\left[\,0\;\;0\;\;\left(-F^{sp}-F^{sh}-F^{sf}\right)\right]^T \tag{30}$$

while the forces acting on the wheel/tire can be expressed as orthogonal components

$$\vec{F}^{\,wt}_{WV}=\left[\,-F^{t}\;\;F^{r}\;\;-F^{n}\,\right]^T \tag{31}$$

in the wheel/tire velocity frame, denoted by F_{WV} with coordinates defined and illustrated in Figure 6. In order to find the virtual work done by $\vec{F}^{wt}_{WV}$ through the virtual displacement δx_p the transformation matrix from F_{WV} to F_{SS}, denoted by $L_{SS\cdot WV}$, is sought. This can be obtained by

$$\begin{aligned} L_{SS\cdot WV} &= L_{SS\cdot RW_1} L_{RW_1\cdot WV} = L_{SS\cdot WH} L_{WH\cdot RW_2} L_{RW_2\cdot RW_1} L_{RW_1\cdot WV} \\ &= L_3(\varphi_{wh})L_1(\phi_{wh})L_2(\theta_{wh})L_3(\beta_{wh}) \end{aligned} \tag{32}$$

then

$$\vec{F}^{wt}_{SS} = L_{SS\cdot WV}\,\vec{F}^{wt}_{WV} \tag{33.a}$$

$$\begin{bmatrix} X^{wt}_{SS} \\ Y^{wt}_{SS} \\ Z^{wt}_{SS} \end{bmatrix} = L_3(\varphi_{wh})L_1(\phi_{wh})L_2(\theta_{wh})L_3(\beta_{wh}) \begin{bmatrix} -F^{sp} \\ F^{\tau} \\ -F^{n} \end{bmatrix} \tag{33.b}$$

The gravitational forces are in a local vertical direction, and also need to be transformed to F_{SS} as follows.

$$\begin{bmatrix} X^{g}_{SS} \\ Y^{g}_{SS} \\ Z^{g}_{SS} \end{bmatrix} = L_{SS\cdot B} L_{B\cdot V} \begin{bmatrix} 0 \\ 0 \\ (m_p + m_{wh} + m_2 + m_3)g \end{bmatrix} \tag{34}$$

The total external moment acting on the wheel axis of rotation is given by

$$M = -M^{bt} + (F^{t}\cos\beta_{wh} + F^{\tau}\sin\beta_{wh})(r_{wh} - \delta_{tire}) \tag{35}$$

Therefore, the total virtual work done by the external forces and moments are

$$\delta W = (-F^{sp} - F^{sh} - F^{sf} + Z^{wt}_{SS} + Z^{g}_{SS})\,\delta x_p + \{-M^{bt} + (F^{t}\cos\beta_{wh} + F^{\tau}\sin\beta_{wh})(r_{wh} - \delta_{tire})\}\delta\mu_{wh} \tag{36}$$

It is important to note that the virtual work done by the gravitational force due to those torque links labeled as 2 and 3 in Figure 6 are not in parallel with the virtual displacement δx_p. The motion of instantaneous center of those torque links, denoted by x_{c_2}, x_{c_3} are related with the x_p as follows. (see Appendix)

$$x_{c_2} = \frac{3}{4}x_p \;,\quad x_{c_3} = \frac{1}{4}x_p \tag{37}$$

Now, evaluating the virtual work Q_1, Q_2 with (29) and (36) results in

$$Q_1 = -F^{sp} - F^{sh} - F^{sf} + Z^{wt}_{SS} + m_p g + m_{wh} g + \frac{3}{4}m_2 g + \frac{1}{4}m_3 g \tag{38.a}$$

$$Q_2 = -M^{bt} + (F^{t}\cos\beta_{wh} + F^{\tau}\sin\beta_{wh})(r_{wh} - \delta_{tire}) \tag{38.b}$$

where

$$Z_{SS}^{wt} = (\cos\phi_{wh}\sin\phi_{wh}\cos\beta_{wh} + \sin\phi_{wh}\sin\beta_{wh})(-F^{sp}) + (\cos\phi_{wh}\sin\theta_{wh}\sin\beta_{wh} - \sin\phi_{wh}\cos\beta_{wh})(F^{r}) + (\cos\phi_{wh}\cos\theta_{wh})(-F^{n}) \tag{38.c}$$

EOM for Telescopic Nose Gear

The motion of telescopic nose gear can be regarded as an dditional degree of freedom in $O_{SS}Z_{SS}$ axis, and the relavant dynamics are well described as a first order system given by

$$T_{\varphi}\dot{\varphi}_{wh} + \varphi_{wh} = K_{\delta_p}^{\varphi}\delta_p + K_{\delta_w}^{\varphi}\delta_w \tag{39}$$

where δ_p, δ_w are rudder pedal and nose wheel tiller deflection angles, respectively, and $K_{\delta_p}^{\varphi}$, $K_{\delta_w}^{\varphi}$ are configuration dependent system constants.

3.4 Transformation to Body Frame

Now that the equation of motion for each gear assembly is derived, the total external forces and moments acting upon the aircraft can be evaluated. For a typical aircraft the landing gear system comprises a telescopic nose gear and wing-body mounted main gears. Equations (26) with (39) applies to all gear assembly while the equation (39) adds to the nose gear assembly. The external forces acting on each gear assembly are conveniently represented in the F_{WV} frame, but these forces need to be transformed into the aircraft body frame F_B so the transformation matrix $L_{B\cdot WV}$ should be found as follows:

$$\begin{aligned} L_{B\cdot WV} &= L_{B\cdot SS}\, L_{SS\cdot WV} \\ &= L_2^T(\vartheta_{ss})L_1^T(-\varphi_{ss})L_3(\varphi_{wh})L_1(\phi_{wh})L_2(\theta_{wh})L_3(\beta_{wh}) \end{aligned} \tag{40}$$

Adding up all the forces from the undercarriage and representing it to the body frame components leads to

$$\begin{bmatrix} F_X^{LG} \\ F_Y^{LG} \\ F_Z^{LG} \end{bmatrix} = \sum_i L_2^T(\vartheta_{ss})L_1^T(-\varphi_{ss})L_3(\varphi_{wh})L_1(\phi_{wh})L_2(\theta_{wh})L_3(\beta_{wh}) \begin{bmatrix} -F^{sp} \\ F^{r} \\ -F^{n} \end{bmatrix} \tag{41}$$

The external moments are now evaluated as

$$\begin{bmatrix} M_X^{LG} \\ M_Y^{LG} \\ M_Z^{LG} \end{bmatrix} = \sum_i \begin{bmatrix} 0 & -z_A^i & y_A^i \\ z_A^i & 0 & -x_A^i \\ -y_A^i & x_A^i & 0 \end{bmatrix} \begin{bmatrix} F_X^{LG} \\ F_Y^{LG} \\ F_Z^{LG} \end{bmatrix} \tag{42}$$

Conclusion

The equations of motion representing an aircraft undercarriage assembly are developed from the first principle. Developed model provides the foundation of carrying out the dynamic analysis and simulation of aircraft motion on the ground. The model is structred; each undercarriage is modeled as mechanical subpart. This also allows to carry out the design of undercarriage system. The second part of this study will present the numerical simulation and the advantages of the developed model.

References

1. Etkin, B., "Dynamics of Atmospheric Flight," John Wiley & Sons Inc., New York, USA, 1970.

2. Hanke, R., "The Simulation of a Large Jet Transport Aircraft, Volume I : Mathematical Model," NASA CR-1756, March 1971.

3. Baarspul Max, "A Review of Flight Simulation Techniques," Progress in Aerospace Science, Vol. 27, 1990, pp. 1-120.

4. Batill, S. M., "A Study of Analytic Modeling Techniques for Landing Gear Dynamics," AFWAL-TR-3027, May 1982.

5. Doyle Jr., G.R., "A Review of Computer Simulations for Aircraft-Surface Dynamics," Journal of Aircraft, Vol. 23, No. 4, 1986.

6. York, B. W. and Alaverdi, O., "A Physically Representative Aircraft Landing Gear Model for Real-time Simulation," AIAA Paper 96-3506, AIAA Modeling and Simulation Technology Conference, San Diego, CA, USA.

7. Pritchard, J. I., "An Overview of Landing Gear Dynamics," NASA/TM-1999-209143, May 1999.

Appendix

Derivation of T_{rel}

• Kinetic Energy of Strut Motion

$$T_p = \frac{1}{2} m_p \dot{x}_p^2 \tag{A.1}$$

where m_p is the mass of the strut assembly.

• Kinetic Energy of Wheel Motion

$$T_{wh} = \frac{1}{2} m_{wh} \dot{x}_p^2 + \frac{1}{2} J_{wh} \dot{\mu}_{wh}^2 \tag{A.2}$$

where m_{wh} is the mass of the wheel assembly, and J_{wh} the mass moment of inertia about the wheel axis of rotation.

• Kinetic Energy of Linkage Members

$$T_2 = \frac{1}{2} m_2 V_{C_2}^2 + \frac{1}{2} J_{C_2} \omega_2^2 \tag{A.3}$$

$$T_3 = \frac{1}{2} J_{O_3} \omega_3^2 \tag{A.4}$$

where m_2 is the mass of the linkage member labeled by 2, J_{C_2} is the mass moment of inertia about the center of mass, C_2, i.e.

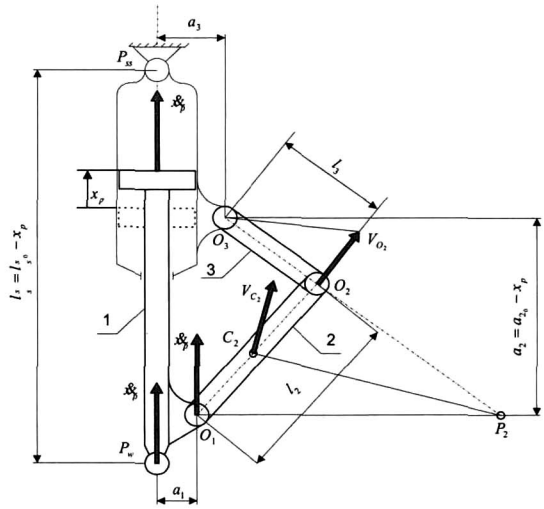

A.1 Linkage Assembly

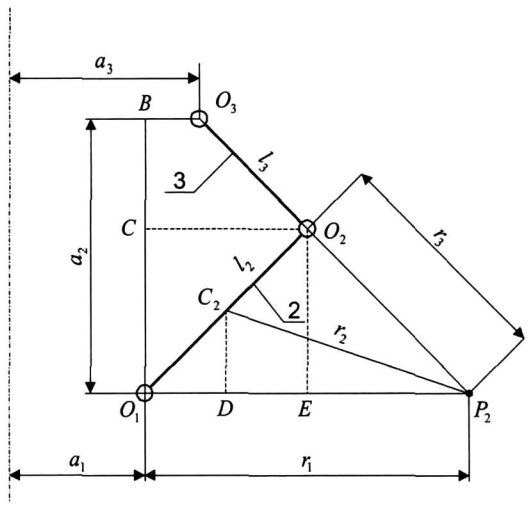

A.2 Linkage Kinematics

$$J_{C_2} = \frac{m_2 l_2^2}{12} \tag{A.5}$$

and V_{C_2} is the velocity of C_2, given by

$$V_{C_2} = \frac{P_2 C_2}{P_2 O_1} \dot{x}_p \tag{A.6}$$

Note that P_2 is the instantaneous center of rotation for the linkage member 2. (refer to Figure A.2) Silimarly, J_{O_3} represents the mass moment of inertia about the O_3 of linkage member labeled by 3, i.e.

$$J_{O_3} = \frac{m_3 l_3^2}{3} \tag{A.7}$$

Let V_{O_2} be the velocity of O_2, then

$$V_{O_2} = \frac{P_2 O_2}{P_2 O_1} \dot{x}_p \tag{A.8}$$

Now, the angular velocities of each member, denoted by ω_2, ω_3, can be obtained from kinematic analysis and given by

$$\omega_2 = \frac{\dot{x}_p}{P_2 O_1} \tag{A.9}$$

$$\omega_3 = \frac{V_{O_2}}{l_3} = \frac{P_2 O_2}{P_2 O_1} \frac{\dot{x}_p}{l_3} \tag{A.10}$$

Let $P_2O_1 = r_1$, $P_2C_2 = r_2$, $P_2O_2 = r_3$, and assuming $a_3 = a_1$ and $l_3 = l_2$ results in

$$r_1 = \sqrt{4l_2^2 - a_2^2} \quad , \quad r_2 = \frac{\sqrt{9l_2^2 - 2a_2^2}}{2} \quad , \quad r_3 = l_2 \tag{A.11}$$

where $a_2 = a_{2_0} - x_p$. Then,

$$V_{C_2} = \frac{\sqrt{9l_2^2 - 2(a_{2_0} - x_p)^2}}{2\sqrt{4l_2^2 - (a_{2_0} - x_p)^2}}\ \dot{x}_p \tag{A.12}$$

$$\omega_2 = \omega_3 = \frac{\dot{x}_p}{\sqrt{4l_2^2 - (a_{2_0} - x_p)^2}} \tag{A.13}$$

Finally, substituing (A.5), (A.6), (A.7), (A.12) and (A.13) into (A.3) and (A.4) yields the relative kinetic energy terms of linkage members, T_2 and T_3.

In (37), the motion of instantaneous center of rotation of linkage members are expressed in terms of x_p, which are obtained from Figure A.3 as below.

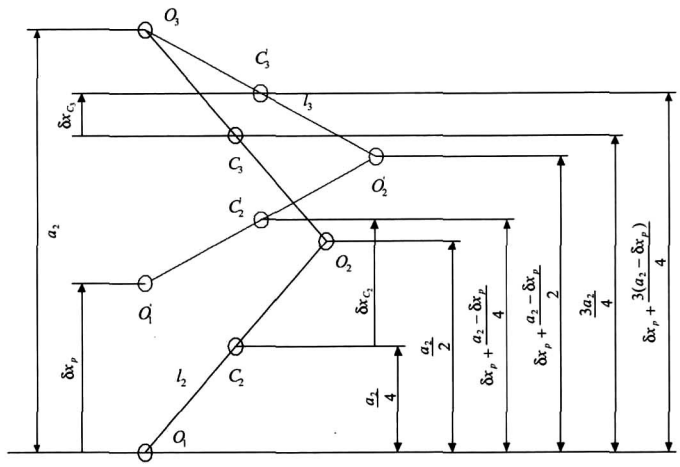

A.3 Linkage Displacements

$$\delta x_{C_2} = \delta x_p + \frac{a_2 - \delta x_p}{4} - \frac{a_2}{4} = \frac{3}{4}\,\delta x_p \tag{A.15}$$

$$\delta x_{C_3} = \delta x_p + \frac{3(a_2 - \delta x_p)}{4} - \frac{3a_2}{4} = \frac{1}{4}\,\delta x_p \tag{A.16}$$